ORIGINAL ARTICLE

Nadim W. Alkharouf · Vincent P. Klink · Imed B. Chouikha · Hunter S. Beard · Margaret H. MacDonald · Susan Meyer · Halina T. Knap · Rana Khan · Benjamin F. Matthews

Timecourse microarray analyses reveal global changes in gene expression of susceptible *Glycine max* (soybean) roots during infection by *Heterodera glycines* (soybean cyst nematode)

Abstract Changes in gene expression within roots of *Glycine max* (soybean), cv. Kent, susceptible to infection by *Heterodera glycines* (the soybean cyst nematode [SCN]), at 6, 12, and 24 h, and 2, 4, 6, and 8 days post-inoculation were monitored using microarrays containing more than 6,000 cDNA inserts. Replicate, independent biological samples were examined at each time point. Gene expression was analyzed statistically using *T*-tests, ANOVA, clustering algorithms, and online analytical processing (OLAP). These analyses allow the user to query the data in several ways without importing the data into third-party software. RT-PCR confirmed that WRKY6 transcription factor, trehalose phosphate synthase, EIF4a, Skp1, and CLB1 were differentially induced across most time-points. Other genes induced across most timepoints included lipoxygenase, calmodulin, phospholipase C, metallothionein-like protein, and chalcone reductase. RT-PCR demonstrated enhanced expression during the first 12 h of infection for Kunitz trypsin inhibitor and sucrose synthase. The stress-related gene, SAM-22, phospholipase D and 12-oxophytodienoate reductase were also induced at the early time-points. At 6 and 8 dpi there was an abundance of transcripts expressed that encoded genes involved in transcription and protein synthesis. Some of those genes included ribosomal proteins, and initiation and elongation factors. Several genes involved in carbon metabolism and transport were also more abundant. Those genes included glyceraldehyde 3-phosphate dehydrogenase, fructose-bisphosphate aldolase and sucrose synthase. These results identified specific changes in gene transcript levels triggered by infection of susceptible soybean roots by SCN.

Keywords *Glycine max* · *Heterodera glycines* · Microarray · Gene expression · OLAP · Soybean cyst nematode · Laser capture microdissection (LCM)

Abbreviations EST: Expressed sequence tag · hpi: Hours post-infection · dpi: Days post-infection · LCM: Laser capture microdissection

N. W. Alkharouf · V. P. Klink · I. B. Chouikha · H. S. Beard
M. H. MacDonald · B. F. Matthews (✉)
USDA-ARS-PSI-SGIL, Bldg.006, Rm 118,
10300 Baltimore Avenue, Beltsville, MD, 20705, USA
E-mail: matthewb@ba.ars.usda.gov
Tel.: +1-301-5045730
Fax: +1-301-5045728

N. W. Alkharouf · I. B. Chouikha
School of Computational Sciences,
George Mason University, Manassas, VA, 20110, USA

N. W. Alkharouf
Department of Cell Biology and Molecular Genetics,
University of Maryland, College Park, MD, 20742, USA

Present address: N. W. Alkharouf
Genome Sciences Centre, BC Cancer Agency, Suite 100,
570 West 7th Avenue, Vancouver, BC, Canada V5Z 4S6,

S. Meyer
United States Department of Agriculture,
Nematology Laboratory, Beltsville, MD, 20705, USA

H. T. Knap
Department of Genetics and Biochemistry,
Clemson University, Clemson, SC, 29634, USA

R. Khan
Graduate School Biotechnology Studies,
University of Maryland University College,
College Park, MD, 20742, USA

Introduction

The soybean cyst nematode (SCN; *Heterodera glycines* Ichinohe) is the major pest of *Glycine max* (soybean) and is responsible for an estimated loss of more than one billion dollars per year in the US (Wrather et al. 2001). This is more than the soybean loss from all other pests

combined. SCN is a sedentary root endoparasite; these nematodes invade the root and partially reorganize root cell function to satisfy their nutritional demands for development and reproduction (Jung and Wyss 1999). After SCN hatch from eggs, they invade soybean roots as infective second-stage juveniles (J2). The J2s are equipped with a robust stylet to cut slits in cell walls to facilitate intracellular migration toward the differentiating vascular cylinder, where they induce their permanent feeding structure, the syncytium (Jung and Wyss 1999). At 18 h after inoculation of roots of soybean cv. Lee, there is a slight enlargement of cells that will form the syncytium (Endo 1991). Within 3 days the syncytium is greatly hypertrophied and several layers of cells are included in the syncytium. The multinucleate syncytium arises from expanding procambial cells whose protoplasts fuse after partial cell-wall dissolution. At the ultrastructural level, syncytia exhibit characteristic features of high metabolic activity, as revealed by hypertrophied nuclei and a remarkable increase in cytoplasmic density accompanied by a proliferation of cell organelles involved in synthesis, transport, and energy supply (Jung and Wyss 1999). Wall ingrowths, characteristic of transfer cells, are formed where these feeding structures contact xylem vessels. The function of these ingrowths is efficient food withdrawal (Grundler and Bockenhoff 1997).

The magnitude of the changes undergone by soybean during syncytium formation and development suggests that a number of genes are involved. Investigators have identified several genes that respond to nematode infection, including extensin (Van der Eycken et al. 1996), catalase (Vaghchhipawala et al. 2001; Niebel et al. 1995), cyclin (Vaghchhipawala et al. 2001; Niebel et al. 1996), β-1,3 endoglucanase (Vaghchhipawala et al. 2001), aldolase and GTP-binding protein (Hermsmeier et al. 1998). Recent investigations using laser capture microdissections (LCM) of soybean syncytia both isolated genes from and demonstrated localized changes in gene expression within syncytia that were extracted from infected tissues (Klink et al. 2005). Thus, the complexity of the soybean–SCN interaction suggests that there are even more genes expressed during the susceptible response of soybean to the nematode infection.

Microarrays have been used to study gene expression changes during cyst nematode parasitism in *Arabidopsis* 3 days post-inoculation to gain a more detailed understanding of the molecular mechanisms underlying the basis of nematode resistance (Puthoff et al. 2003). In that study changes in mRNA levels were examined in *Arabidopsis* after infection with two species of nematodes, the sugar beet cyst nematode (BCN; *Heterodera schachtii*) and the soybean cyst nematode (SCN). *Arabidopsis* is susceptible to BCN. However, SCN cannot establish themselves in *Arabidopsis*. Microarrays have also been used to study gene expression in plants under abiotic stress and other treatments, including drought, cold, diurnal cycling, salt, temperature, oxidative stress, small signaling molecules such as salicylic acid and methyl jasmonate, and several biotic stresses (Reymond et al. 2000; Kiegle et al. 2000; Schenk et al. 2000; Schaffer et al. 2001; Kawasaki et al. 2001; Seki et al. 2001; Oztur et al. 2002). However, no study has attempted to examine the gene expression changes of susceptible soybean roots during cyst nematode infection over a period of several days.

In this paper, we analyzed gene expression in roots of *G. max* cv. Kent, susceptible to SCN population NL1-RHp over seven time-points ranging from 6 h post-infection (hpi) to 8 days post-infection (dpi) by SCN, using microarrays containing over 6,000 cDNA inserts specifically isolated from soybean roots. Our results show that the abundance of transcripts of numerous soybean genes change in susceptible roots when examined during the migration phase of SCN infection at 6 and 12 hpi compared to those expressed at 6 and 8 dpi. These later time-points coincide with when many of the nematodes have established their feeding site.

Materials and methods

Plant and nematode materials and RNA isolation

Plant and nematode materials were grown as described previously (Khan et al. 2004). Briefly, Kent (susceptible) seeds were surface sterilized, and then germinated on water agar plates for 3 days at room temperature in the dark. Eggs from SCN, *H. glycines* population NL1-RHp, which infects as Race 3 in differential screening, were incubated in sterile water at room temperature on a rotary shaker at 25 rpm to promote hatching. After 2 days the juveniles were collected and concentrated by centrifugation to approximately 3,000 J2/ml. Using a method similar to Hermsmeier et al. (1998), 20 radicals were excised and placed in a pinwheel formation with the root tips pointing inward on a circle of sterile Whatman 3 mm paper on top of Gamborg's B5 media (GIBCOBRL, Gaithersburg, MD, USA) in Petri dishes. Replicate experiments using different isolations of J2 nematodes and *G. max* cv. Kent seeds were repeated in their entirety at different times. Petri dishes, each containing 20 roots, were set up for the experiments. Each set of 20 roots was inoculated with 3,000 J2s in sterile water. The control replicates received the same volume of sterile water. After 6 and 12 hpi, and 1, 2, 4, 6, and 8 dpi of exposure to the nematodes, the roots of both mock-treated and infected roots were rinsed in deionized water to remove any debris and J2s that had not infected the roots. The tissue was then flash-frozen in liquid nitrogen. The frozen root tissue was ground to a fine powder using a mortar and pestle chilled in liquid nitrogen. Total RNA was extracted using the method of Mujer et al. (1996). The yield was typically 300 μg of total RNA/g of wet tissue.

cDNA microarray clones and microarray fabrication

cDNA clones from four different libraries were used in assembling the microarray. The first library was

constructed from Peking and PI437654, soybean genotypes resistant to SCN population NL1-RHp. The Peking Lambda ZAP II cDNA library was made with mRNA from the roots and shoots of Peking plants, 48 h after the nematode infection, according to the manufacturer's instructions (Stratagene; La Jolla, CA, USA). A total of 1,000 clones from this library, with an average insert size of 1,000 bp, were used in assembling the microarray. Each clone was sequenced with a vector primer at the 5′-end of the insert, and the sequence detected on an ABI Prism 3100 sequencer.

The second and third libraries were suppressive subtraction libraries prepared from roots of PI437654 as described in Tomkins et al. (1999). Briefly, in those experiments, uninfected plants (control) were mock inoculated with distilled water. Root segments, 2–3 cm from the elongation zone, were harvested at 34 h after the initial inoculations from both infected and uninfected seedlings. Isolation of infected and control root mRNA was performed using mRNA Fast Track Isolation Kit (Invitrogen; Carlsbad, CA, USA). For the suppression subtractive hybridization procedure, about 2 g root tissue was used. For the forward subtraction, SCN-infected seedling mRNA served as a tester. Uninfected plant mRNA formed the driver. Conversely, for the reverse subtraction, uninfected seedling mRNA served as a tester and the driver was infected plant mRNA. cDNA synthesis, adaptor ligation, hybridizations, and PCR amplifications were done according to the procedures of the suppression subtractive hybridization kit (Clontech; Palo Alto, CA, USA). Approximately 2,500 clones from those libraries were used in assembling the microarray.

The fourth library contained approximately 2,500 clones and was obtained from E.I. Dupont de Nemours and Co, Newark, DE, USA. These proprietary clones were individually selected from several libraries, because they were known to have a function in the plant defense response.

Nucleotide sequences and predicted amino acid sequences, for all cDNA clones in the four libraries, were compared against those in Genbank, EMBL, and Swiss Prot databases using BLAST tools (Altschul et al. 1997). Although some redundant clones were removed after being identified through pairwise comparison of each clone against the EST database housed at the USDA-ARS-Beltsville Soybean Genomics Microarray Database (SGMD; Alkharouf and Matthews 2004) many clones in this microarray are redundant.

The confirmed clone inserts were amplified by T3/T7-primed polymerase chain reaction (PCR) in a 96 well microtiter plate using a PTC 225 thermocycler (MJ Research; Waltham, MA, USA) with protocols adapted from Hegde et al. (2000). Excess primers and unincorporated nucleotides were removed by ethanol precipitation in the presence of 2 M ammonium acetate. The amplified product from each clone was checked on a 1% agarose in $1\times$ TBE gel for the presence of a single band, and brought to a final volume of 5 μl in 50% DMSO 50% TE solution.

The standard reference design was used for these microarray experiments; the reference (control) sample was RNA extracted from soybean roots not infected with SCN, and the treatment samples were RNA extracted from Kent (SCN-susceptible) cultivars at 6, and 12 hpi, and 1, 2, 4, 6, and 8 dpi with SCN. Dye swaps were used to correct for differences in incorporation and fluorescent properties of two dyes, Cy3 and Cy5. Two replicated slides were used for each time-point, one of which is the dye swap, generating a total of 14 slides per biological experiment. Two biological experiments were used to account for the inherent variation in mRNA extracted from different plant materials. Six self–self-hybridized slides were also generated for T-test analysis, wherein a pool of RNA was split into two aliquots, one labeled with Cy3 and the other labeled with Cy5, and then hybridized to the slide. The complete list of slides printed and the probes used in their hybridization are listed on our web site [http://www.psi081.ba.ars.usda.gov/SGMD/Publications/KentTmeline/].

The PCR products suspended in 50% DMSO/TE at a concentration of 0.4 μg/ml were arrayed from a 96-well microtiter plates onto silylated Corning CMT-GAPs microscope slides. Each clone was printed in triplicate as described previously (Khan et al. 2004) using a Cartesian robot model PixSys 5500 PA workstation with a telechem printing head and Stealth quill pins. A total of 6,543 soybean cDNA clones were arrayed. cDNAs from alfalfa weevil were printed at concentrations of 1, 2.5, 5, 10, 25, 50, and 100 μg/ml to serve as internal controls, and to assess for labeling and detection efficiencies. The printed arrays were cross-linked to the slide by UV irradiation at 250 mJ using UV Stratalinker 2400 (Stratagene). The slides were stored in a humidity chamber at 25°C.

Fluorescent probe preparation

Total RNA from each sample was labeled using the reverse transcription reaction as described by Hegde et al. (2000) with few modifications (Khan et al. 2004). Three specific control poly (A)$^+$ RNAs (pλ11-3; pml-72; Sp3) corresponding to coding sequences from alfalfa weevil, cow, and human DNA, respectively, were synthesized by in vitro transcription as described (Khan et al. 2004).

Microarray hybridization and analysis

The cDNA used for the hybridizations was obtained from independently run experiments. The arrays were prehybridized, hybridized, washed, and dried as described (Khan et al. 2004). Microarrays were scanned for each fluorophore at a resolution of 10 μm, and a PMT and laser power set to 70, using ScanArray 4000 (GSI Lumonics; Meriden, CT, USA).

Fluorescence intensities were extracted from the scanned images using the image processing software package SPOT which is available at http://www.cmis.csiro.au/ iap/spot.htm. Background subtraction

was performed before calculating ratios. The elements with either printing or hybridization artifacts were flagged and discarded before analysis. Only spots with an intensity of at least 1.5 times above the local background in both channels were used for subsequent analysis. This filtering process usually removed 5–15% of the elements, the percentage of which varied from slide to slide. The extracted data from each slide were then log transformed (using log base two) and normalized using the Lowess print-tip group normalization method (Yang et al. 2002).

Potential artifacts and false positives were eliminated by selecting for further analysis only those clones that exhibited similar expression patterns between the original hybridization and their dye swaps (Yang et al. 2002). These clones were determined by the one-way analysis of variance (1-ANOVA) tests, which were used as a tool to detect similar expression levels across replicated slides and across the two biosamples (Bilban et al. 2002). Only clones with an F-value high enough to produce a probability of 0.1 or lower were selected as being similar across biosamples. SQL procedural scripts were written to conduct such computationally intense calculations for every clone post-filtration and normalization. In general there was little variation between the two biosamples.

T values on $\log_2$ expression ratios were calculated using Student's T-test to identify genes with statistically significant expression ratios. Self–self-hybridized slides with equal amounts of cy3- and cy5-labeled RNA from uninfected Kent (K−/K−) were used as control groups for the T-test. Most of the clones printed in K−/K− show a ratio close to one after Lowess print-tip normalization.

T-tests were used to analyze the expression of each clone in SCN infected Kent versus uninfected Kent (K+/K−) using background corrected and normalized expression ratios. Genes that had large absolute T-statistic values and positive average expression levels were considered differentially induced genes, while genes that had large absolute T-statistic values but negative average expression levels were considered differentially suppressed genes.

Results of T-tests were used to determine significance ($P \leq 0.05$) of gene induction and gene suppression. If the gene induction or suppression passed the T-test, then a cutoff value of 1.5-fold induction or suppression was applied for extra stringency. The high stringency criteria keep the possibility of false positives to a minimum but at the same time increase the likelihood of false negatives (genes actually induced but are not designated as such). This statistical method takes into account the variability within slides and between replicated slides as well as biological samples to distinguish gene expression changes caused by treatments from gene expression changes attributable to biological and measurement variability. The use of arbitrary fold changes may be misleading and result in false interpretations (Puthoff et al. 2003).

The results of the T-test were compared with those from using significant analysis of microarrays (SAM) as described in Tusher et al. (2001). SAM identified an average of 25% more genes differentially expressed than our T-tests using the one class method, which conducts a T-test after calculating a set of data permutations. The underlying assumption in the one class SAM method is that genes have a fold induction of 1 (unchanged) before treatment. The self–self-hybridized slides, however, give a better estimate of fold induction before treatment. We identified a number of genes with fold induction values of 1 ± 0.25 in the self–self-hybridized slides due to the variability inherent in microarray experiments. The T-test accounts for this variability but SAM does not. Differential genes determined by T-tests were generally a subset of SAM's differential gene list.

Genes were classified into functional categories based on their mapping with the gene ontology (GO) database. The GO database (The gene ontology consortium, 2004) was downloaded and custom SQL scripts were written to map the putative gene names with that of the GO terms. Genes were subsequently categorized based on what higher-level molecular function and/or biological process they best relate.

SQL and online analytical processing (OLAP; Codd et al. 1993; Alkharouf et al. 2004) were used to produce lists of differentially expressed genes in each of the time-points. In addition the clustering function within Analysis Services (Microsoft; Redmond, WA, USA) was used to find distinct expression profiles in the differentially expressed genes.

RT-PCR

RT-PCR was performed on *G. max* cv. Kent roots that were either uninfected, or infected for either 12 or 196 h (8 days) with *H. glycines* isolate NL1-RHp. Aliquots of RNA for the uninfected roots, or roots infected for either 12 or 196 h with *H. glycines* respective to samples used in the microarray analyses were used as templates for RT-PCR. The cDNA was obtained from separate experiments as previously mentioned. RNA was converted to cDNA according to Klink et al. (2005) using Superscript First Strand Synthesis System for RT-PCR (Invitrogen) using an oligo d(T) as a primer according to the manufacturer's directions. Primer pair oligonucleotides designed from the corresponding EST nucleotide sequences and their amplicon length can be found in Table 2. Relative quantities of gene expression were determined using the Stratagene Mx3000P Real-Time PCR system (Stratagene) using the manufacturer's directions. DNA accumulation during the reaction was measured with SYBR Green with ROX as the reference dye. RT-PCR of genes was performed with serial dilutions over a five-log range. PCR efficiencies were equal in each case. The C_t values and relative abundances of RNAs from our experiments were calculated using Stratagene Mx3000P software Real-Time PCR system. As controls, we compared the expression values to EIF3 (CA852991) and S21 ribosomal protein S21 (CF921751). Other controls for RT-PCR had included reactions containing either no template or RNA processed with no Superscript reverse transcriptase. Both gel electrophoresis

and the SYBR Green dissociation curve of amplified products demonstrated the production of a single product per reaction. DNA for the RT-PCR was dissociated for 10 min at 96°C, followed by PCR cycling and temperatures set for denaturation for 30 s at 96°C, annealing for 60 s at 55°C and extension for 30 s at 72°C. RT-PCR data were obtained by averaging the normalized expression ratios for both EIF3 and S21 ribosomal protein controls

Results

Whole tissue mount timecourse of *H. glycines* infection of *G. max* roots

During the early time-points (6 and 12 hpi) the SCN penetrates the soybean root and migrates toward the vascular cylinder (Fig. 1). At 18 h of infection and beyond, the nematode typically selects a pericycle or endodermal cell as a feeding site that will expand later to merge with adjacent cells and become the syncytium (Endo 1964, 1965, 1971, 1991). Because SCN infection and migration is not synchronous, we refer to 6 and 12 hpi as the early time-points wherein SCN penetrates the root and migrates to find a feeding site. The mid-time-points (1, 2, and 4 dpi) are when syncytia are formed and nematode feeding begins. At the later time-points 6 and 8 dpi numerous syncytia are already established and continue to expand; nematode growth is evident by the increase in nematode diameter (Fig. 1f, g).

Timecourse microarray analyses of *H. glycines* infections of *G. max* roots

We examined changes in the abundance of gene transcripts at each of the seven time-points in duplicate biological replicates using microarrays that contained over 6,000 cDNA inserts that were selected specifically from soybean root cDNA libraries to target root response. Total RNA was isolated from roots at 6 and 12 hpi, and 1, 2, 4, 6, and 8 dpi with SCN and from uninfected roots, serving as the control, for duplicate hybridizations to microarrays using inverse labels (dye swaps). Variation within and across microarray slides after Lowess print-tip group normalization was examined to ensure correct normalization and confirm that reproducibility was good. Very little variation occurred within slides with approximately 85% of the clones having standard deviations of less than 0.5 times the mean ratio after filtration and normalization. Across slide variation was low and the reproducibility was high when data from biological replicates and dye swaps were compared at 6 and 12 hpi, 1 and 2 dpi (Fig. 2) and at 4, 6, and 8 dpi (Fig. 3) as documented by the box plots. Variation and reproducibility was examined in triplicate using aliquots of uninoculated control RNA for self–self-hybridizations, wherein two aliquots of the same RNA were each labeled with a different dye, and then hybridized to a microarray. Therefore, the resulting ratios for each feature on the microarray should be equal to one. Variation from a ratio of one reflects differences in printing, labeling, hybridizing, and other technical aspects of the experimental system and can be used in *T*-test comparisons (Fig. 3d).

Fig. 1 Micrographs showing SCN infection progression in *Glycine max* cv. Kent roots that were infected with *Heterodera glycines* and grown for defined times. **a** 6 hpi, **b** 12 hpi, **c** 1 dpi, **d** 2 dpi, **e** 4 dpi, **f** 6 dpi, and **g** 8 dpi
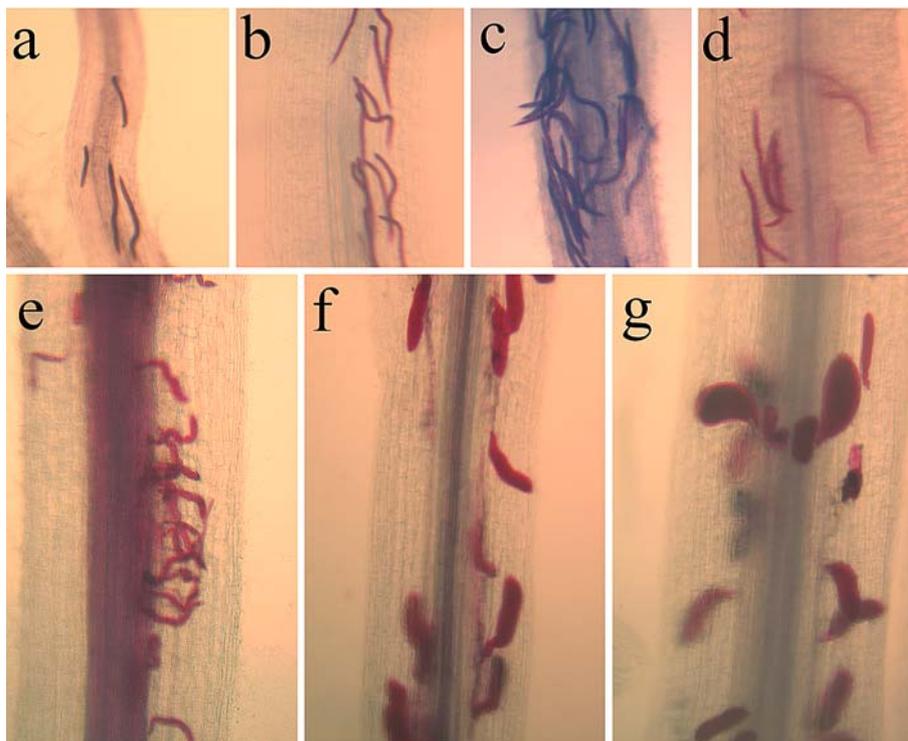
Fig. 2 *Box plots* showing the variation between a slide and the corresponding dye swap for both biological sample 1 (*y*-axis *1* and *2*) and biological sample 2 (*y*-axis *3* and *4*) in K+/K− for each time-point. Time-points 6, 12 hpi, and 1 and 2 dpi are shown. Note the change in scale of the *x*-axis, for **b** and **c**
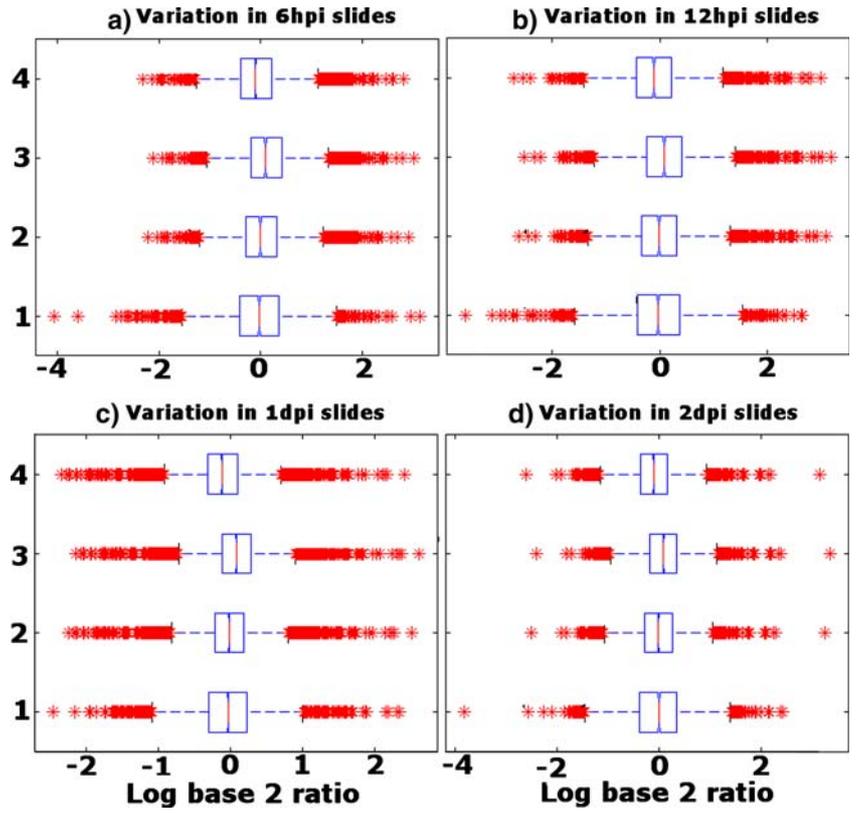

Fig. 3 *Box plots* showing the variation between a slide and the corresponding dye swap for both biological sample 1 (*y*-axis *1* and *2*) and biological sample 2 (*y*-axis *3* and *4*) in K+/K−, for each time-point. Time-points 4, 6, 8 dpi are shown. Also shown in **d** is the variation in the self–self-hybridized slides (K−/K−) for biological sample 1 (*y*-axis *1*, *2* and *3*) and biological sample 2 (*y*-axis *4*, *5* and *6*). Note the change in scale of the *x*-axis, especially for **d**
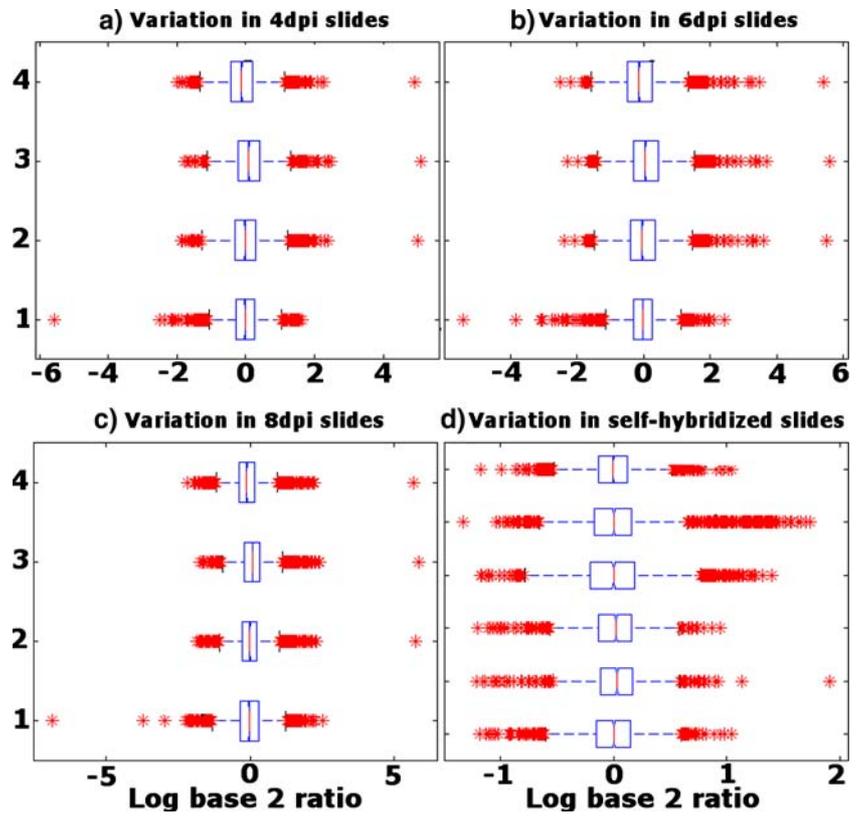
The number of differentially expressed genes at each time-point after T-tests ($P \leq 0.05$) is provided in Fig. 4. The number of differentially induced genes above 1.5-fold ranged from a low of 61 at 1 dpi to 287 at 6 dpi. Approximately 190 genes, on average, were induced at any point over the timecourse. Similar results were obtained for differentially suppressed genes below -1.5-fold, ranging from a low of about 128 genes suppressed at 12 hpi and 1 dpi and over 243 genes suppressed at 6 dpi.

The putative protein names for all differentially expressed genes were mapped to the gene ontology consortium database (The gene ontology consortium 2004) for functional categorization purposes as depicted in Fig. 5. Even though the majority of the genes, 45–55%, have unknown and/or unclassified functions based on the gene ontology mappings, the results show changes in the percentage of genes belonging to certain functional categories over the measured time-points. The percent induced genes involved in protein synthesis for instance, is increased at 4 and 6 dpi, while percentage of genes involved in signal transduction are increased at 6 hpi through 1 dpi and then later at 8 dpi. Stress-/defense-related genes increase at 1 and 2 dpi, and genes involved in cell structure (specifically cell wall structure) are increased at 12 hpi and 1 dpi, corresponding to the time when SCN is actively migrating toward the root stele and forming the syncytium. Metabolism-related genes stay fairly constant during the early and mid-time-points with a slight dip in the later time-points. Most of the other functional categories do not show much variation across the measured time-points.
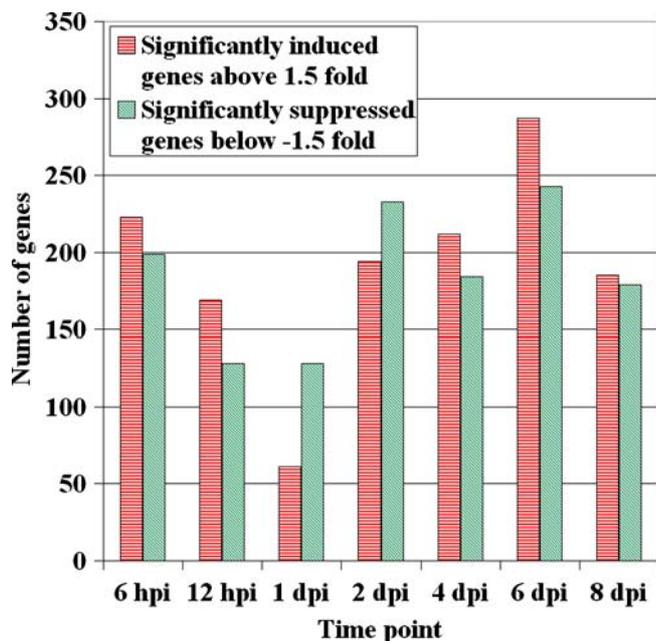
SQL queries and OLAP (Alkharouf et al. 2005) were used to produce lists of differentially expressed genes at each of the seven time points. These lists were then fed into the clustering algorithm of Analysis Services, which ships with SQLServer2000 (Microsoft). The clustering algorithm was used mainly to graphically view the results of OLAP and come up with groups of genes with distinct expression profiles. Four distinct expression profiles resulted from this analysis; they are shown in Fig. 6.

The first profile (profile 1 in Fig. 6) represents a number of genes that were commonly induced ($P \leq 0.05$ and 1.5-fold and above) during the early time-points of infection (6 and 12 hpi; Table 1). In addition, these genes were found not induced at the later time-points as determined by OLAP queries. Among these genes were Kunitz trypsin inhibitor (KTI), genes encoding stress-related proteins, SAM-22 (a stress-induced PR-10 protein); germin-like protein, probable 12-oxyphytodienoate reductase, trehalose-6-phosphate synthase (TPS) homolog, phospholipase D, and several genes encoding enzymes in the phenylpropanoid pathway, including 6′deoxychalcone synthase, 4-coumarate CoA ligase, and chalcone reductase.

The second profile (profile 2 in Fig. 6) represents genes differentially induced ($P \leq 0.05$) at the later time-points (6 and 8 dpi). Profile 2 included transcripts of genes encoding proteins involved in transcription, translation, and protein folding, including numerous initiation factors, 60S, 40S, 20S ribosomal proteins, calnexin, and peptidylprolyl isomerase. Similarly, transcripts of genes encoding enzymes in glycolysis and carbon metabolism were more abundant, including those elevated and encoding fructose-bisphosphate aldolase, glyceraldehyde dehydrogenase, sucrose synthase, fructokinase and malate dehydrogenase, as well as transcripts encoding a sucrose transport protein and a triose phosphate translocator. Transcripts of calcium-related genes, calmodulin, annexin, and calnexin, were also elevated (Table 1).

The third profile (profile 3 in Fig. 6) included genes that were differentially induced across most or all the time-points. These included polyubiquitin, metallothionein, calmodulin, phospholipase C, lipoxygenase, CLB1, Skp1, and the WRKY transcription factor (Table 1).

The final profile (profile 4 in Fig. 6) included genes that were differentially suppressed across the time-points. These included a large number of unknown genes and genes encoding putative proteins, as well as signal transduction gene S-receptor kinase and photosynthesis-related cytochrome P450 (Table 1).

RT-PCR analyses

We wanted to confirm by an independent means the expression trends we observed on the microarrays. We performed RT-PCR for seven genes. These ESTs encoded homologs of WRKY (BM108156), TPS (DUP06H06), EIF4a (BM108249), SKP-1 (BM108118), CLB-1 (BM108106), KTI (CA852010) and sucrose synthase (BM107809). As controls, we used both EIF3 (CA852991) and ribosomal S21 (CF921751; Table 2).
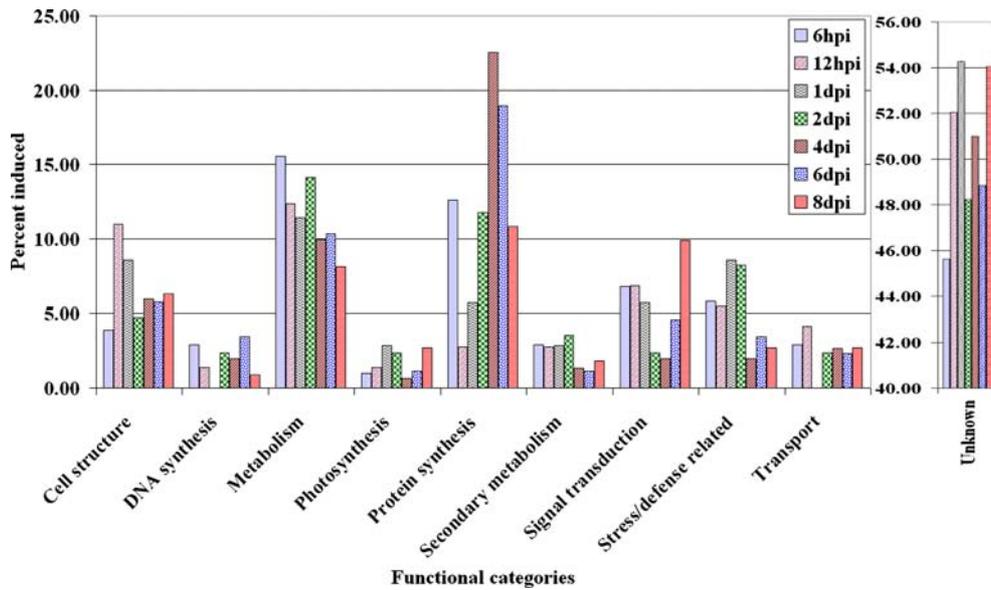

Fig. 4 The number of differentially expressed genes after T-tests ($P \leq 0.05$) at each time-point using a cutoff value of 1.5-fold for extra stringency and selecting for clones that have standard deviations of less than or equal one times the mean expression ratio

Fig. 5 Functional categorization of differentially induced genes in soybean roots at each of the seven time-points after infection with SCN. The percentage of induced genes at each functional category was calculated based on the number of genes involved in that function over the total number of differentially induced genes in the specific time-point. Genes were classified in their respective categories after being mapped to the gene ontology database as described in Materials and methods. The number of protein synthesis genes is increased at 4 and 6 dpi, while signal transduction genes are increased at 6 hpi through 1 dpi and then later at 8 dpi. Metabolism-related genes stay fairly constant during the early and mid-time-points with a slight dip in the later time-points. Stress/defense-related genes increase at 1 and 2 dpi corresponding to the time when SCN is actively burrowing and forming the syncytium. A majority of the induced genes, 45–55%, are unknown and/or have no functional classification based on the gene ontology mappings

Fig. 6 Expression profiles of genes differentially expressed in soybean roots after infection with SCN. The expression ratios were calculated from normalized, rescaled ratios of the fluorescence intensity in the red and green channels. Ratios represent the average from the two biological samples that' were used. *Error bars* show the standard deviation of expression levels at each time-point. *Profile 1* represents genes induced at the early time-points (6 and 12 hpi). *Profile 2* represents genes induced at the later time-points (6 and 8 dpi). *Profile 3* represents genes differentially induced over time, while *profile 4* represents genes differentially suppressed over time
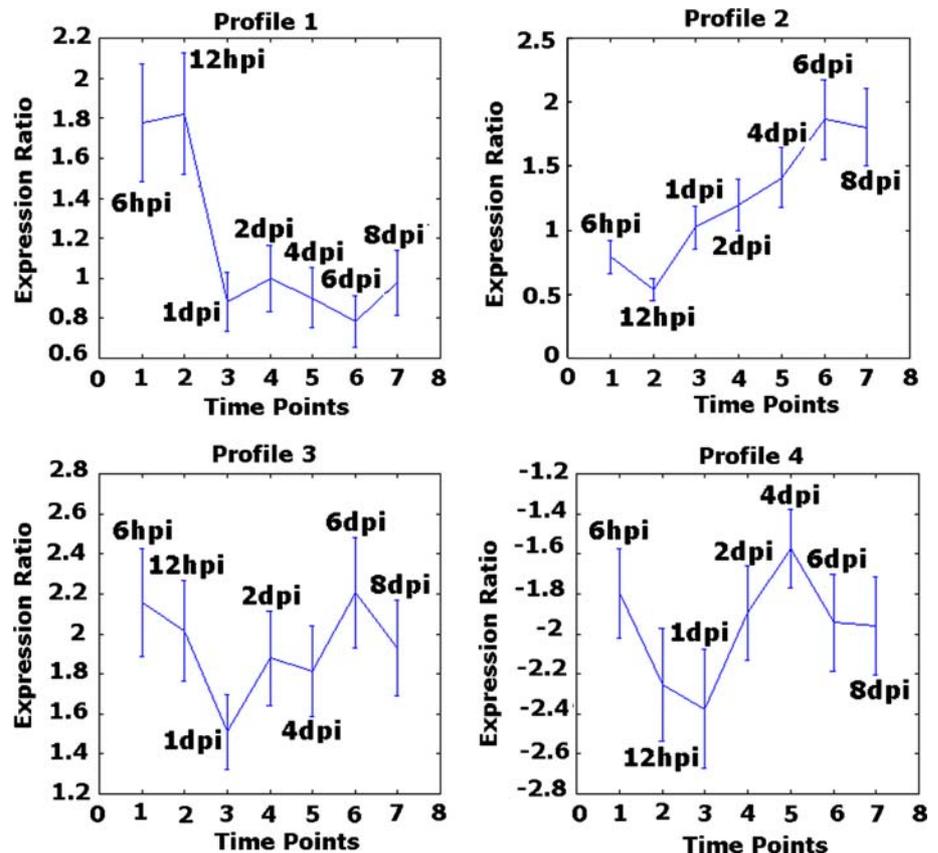
Table 1 Select genes from profiles 1 through 4 in Fig. 6 that showed differential expression in soybean roots *G. max* cv. Kent against SCN infection. The cut off value for these genes was a threshold of 1.5 (please refer to Materials and methods section for details). Thus, these genes are threshold of ±1.5

Profile, functional category, Genbank ID	Putative protein name[a]	Putative function
Profile 1		
Stress/defense related		
BM107871; BM108178	SAM22 (PR-10)	Pathogenesis related
CA852010	Kunitz trypsin inhibitor	Pathogenesis related
BM107847	Germin-like protein	Anti-microbial activity
BM139851	Stress-induced gene	Stress related
BM108184	Peroxidase (EC 1.11.1.7) precursor	Stress related
BM108004; BM108178	Phospholipase D	Stress related
BM107976	Probable 12-oxyphytodienoate reductase	Stress related
Metabolism		
DUP06H06	Trehalose-6-phosphate synthase homolog	Trehalose synthesis
Secondary metabolism		
BM108022	4-Coumarate CoA ligase	Ligase activity, involved in secondary metabolite synthesis
BM107806	6′Deoxychalcone synthase	Phenylpropanoid pathway
BM108162	Chalcone reductase	Phenylpropanoid pathway
Cell structure		
BM139577	Repetitive proline-rich protein	Cell wall structure
Profile 2		
Stress/defense related		
BM108262; BM107930	Heat shock protein 90, 70	Protein degradation
CA853292	Peroxidase	Detoxification
Protein synthesis		
BM108251; CA853701; BM108211; BM107991; CA852078; CA852610; BM107813	60S, 40S, 20S ribosomal proteins	Translation
CA853657	Peptidylprolyl isomerase	Protein folding
BM108249	Initiation factor 4A-15	Translation
CA852991	Translation initiation factor 3	Translation
Metabolism		
BM108246; CA852009	Fructose-bisphosphate aldolase	Sugar metabolism
BM108242	Glyceraldehyde 3-phosphate dehydrogenase	Sugar metabolism
BM107809; CA853158	Sucrose synthase	Sugar metabolism
CA853806	Fructokinase	Sugar metabolism
CA851978	Malate dehydrogenase	Sugar metabolism
BM107917	Calmodulin	Calcium related
CA853555	Annexin	Calcium related
BM107760	Calnexin	Calcium related
Transport		
BM108083	Sucrose transport protein	Sucrose transport
BM108309	Triose phosphate translocator	
Profile 3		
Stress/defense related		
BM108088	Phospholipase C	Synthesis of antifungal phytooxylipins
BM108224	Calmodulin	Defense response
BM108228	Metallothionein	Membrane channeling
BM108011; BM108233	Lipoxygenase	Wound response, jasmonic acid biosynthesis
BM108156	WRKY transcription factor	Defense response
BM108106	CLB1	Membrane channeling and signaling
BM108118	Skp1	Protein degradation
Secondary metabolism		
BM107806	Chalcone reductase	Phenylpropanoid pathway
BM107798	4-Coumarate CoA ligase	Ligase activity, involved in secondary metabolite synthesis
Profile 4		
Unknown\unclassified		
CA850695; CA850508; CA851253; A851269	Unknown protein	Unknown
Signal transduction		
CA853083	S-receptor kinase	Kinase activity
Photosynthesis		
BM107683	Cytochrome P450	Electron transport

[a] Based on Blast N or Blast X best hits with significant *e*-values

Using uninfected roots as our reference tissue for RT-PCR, we observed increases in expression for WRKY, TPS, EIF4a, SKP-1, and CLB-1 between uninfected roots and roots infected for 12 h (Fig. 7). We then compared those same genes by RT-PCR between the uninfected roots and roots infected for 196 h (8 dpi) showing that those genes become even more highly expressed (Fig. 7). However, the decreases in expression that were observed on microarrays between the 12 h and 8 dpi samples for WRKY6 and TPS appeared as increases on RT-PCR experiments. For both KTI and sucrose synthase, RT-PCR demonstrated initial increases in expression between uninoculated roots and roots infected for 12 h (Fig. 7). However, RT-PCR revealed that KTI exhibited a dramatic decrease in expression between 12 hpi and 8 dpi, confirming our microarray data. RT-PCR demonstrated that sucrose synthase levels experienced a slight decrease in expression between 12 hpi and 8 dpi. Our RT-PCR data corroborate the relative expression trends of the respective genes obtained by our microarray analyses.

Discussion

Timecourse microarray analyses of *H. glycines* infection of *G. max* roots provide a useful database of global gene expression

We analyzed gene transcript levels in susceptible soybean roots at 6, 12 hpi, and 1, 2, 4, 6, and 8 dpi after infection of soybeans by the SCN. These analyses provide extensive data on the expression of a large number of soybean genes during critical periods of infection, wherein SCN migrates through the root and establishes a feeding site. More detailed information concerning these genes can be found at our web site [http://www.psi081.ba.ars.usda.gov/SGMD/Publications/KentTmeline/]. Our data confirm gene expression data of numerous other researchers examining gene expression in roots at single time-points during the nematode infection. (Mahalingam et al. 1999; Vaghchhipawala et al. 2001, 2004; Gheysen and Fenoll 2002; Puthoff et al. 2003; Khan et al. 2004; Klink et al. 2005). Our data extend their observations by measuring expression of these and thousands more genes at numerous time-points during the cyst nematode infection and feeding, rather than at one or a selected few time-points. Our analyses extend our understanding of root infection by expanding the microarray analysis to include time-points at 6, 12, and 24 h, times prior to syncytium initiation. However, while the microarrays developed for this study were not composed of cDNAs obtained from *G. max* cv. Kent tissues, all of the mRNA used for the experiments were obtained from Kent. Our RT-PCR experiments that do not rely on hybridization to non-Kent cDNA are consistent with the microarray data. Similar microarrays generated from multiple soybean germplasm sources have been shown to provide useful data that is sufficiently reliable to compare isogenic lines that differ with respect to a mutant phenotype (Vodkin et al. 2004). Thus, those microarrays from heterologous sources were able to define a small list of candidate genes that may correspond directly to that mutant phenotype

Table 2 PCR primer pairs used for RT-PCR

The Genbank match is provided in parentheses beside each gene and the amplicon length is provided in base pairs. The primary sequence of the gene data for each amplicon was obtained by re-sequencing the DNA sequence from cDNA. From those data, PCR primers were designed and used for RT-PCR

EST	Amplicon length (bp)
BM107809 (sucrose synthase)	
Upper: 5′-CGGCGGCAAGAAACTCCTC-3′	76
Lower: 5′-AACTTGGCACGTGTGGCAGATA-3′	
CA852010 (Kunitz trypsin inhibitor)	
Upper: 5′-TCAAACTCACTGGCTACAAAAACA-3′	122
Lower: 5′-ATCCCCACACGAACTATCATCATT-3′	
BM108106 (CLB-1)	
Upper: 5′-TGGTGATAATTTGCCTGAGTGGAT-3′	109
Lower: 5′-CATGGTTGCTGCTTCTGCTACA-3′	
BM108118 (Skp1)	
Upper: 5′-CGGTGGCGCTGGAGTCG-3′	70
Lower: 5′-AGAGGGATGCCGCTGTCG-3′	
BM108156 (WRKY)	
Upper: 5′-ACTTCGCATTCCCATTCTTCGTC-3′	99
Lower: 5′-ATCACTAGCACCCCCATTCTTCTT-3′	
BM108249 (EIF4A-15)	
Upper: 5′-CTGGAACTGGGAAGACGGCTACT-3′	134
Lower: 5′-TGCTCGCATAACCTTCTCAATCTG-3′	
DUP06H06 (trehalose phosphatase-synthase)	
Upper: 5′-AGCGCACTTGTCGTTTCTGAG-3′	67
Lower: 5′-GGTTTACCCTTATTGCCCCACTA-3′	
CF921751 (ribosomal-S21)	
Upper 5′CTAAGATGCAGAACGAGGAAGG	168
Lower 5′GAGAGCAAAAGTGGAGAAATGG	
CA852991 (EIF3)	
Upper: 5′-TTTGTGTTGCTGATGCCTCTTTTT-3′	109
Lower: 5′-AGGCAACACCATCACATACCATAA -3′	

Fig. 7 RT-PCR of genes differentially expressed in soybean roots after infection with SCN. We performed RT-PCR of homologs of WRKY, TPS, EIF4a, SKP-1, CLB-1, KTI, and sucrose synthase. RT-PCR data were obtained by averaging the normalized expression ratios for both EIF3 and S21 ribosomal protein controls. We used uninfected roots as our reference tissue and compared expression to roots infected for 12 h or 8 days (refer to Materials and methods)
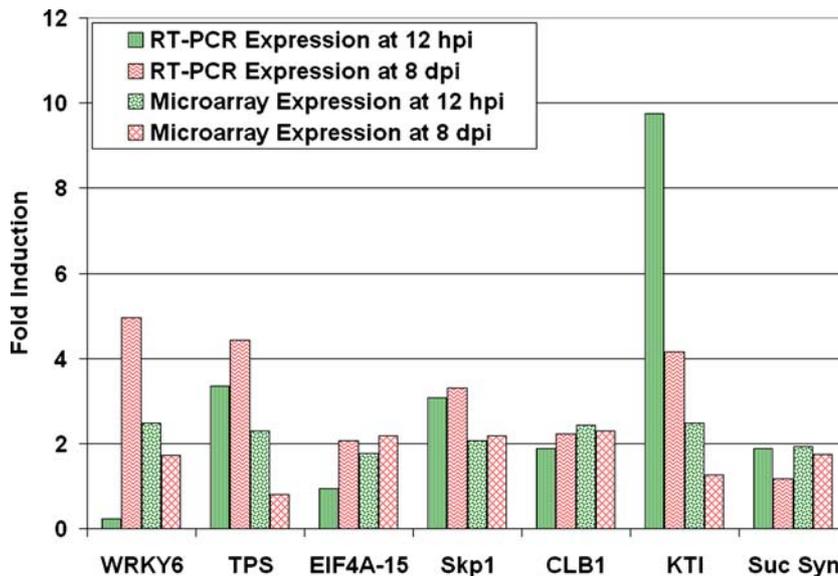
(Vodkin et al. 2004). Therefore, we believe that the use of non-Kent cDNAs to construct our microarrays probably do not adversely affect the hybridization outcome in most cases and are revealing the expression trends occurring within the infected Kent root tissue.

Our data analyses identified many genes elevated during nematode migration even before feeding began. Our study has identified genes expressed at later time-points during infection when feeding sites are established. A surprising outcome was an apparent global suppression of gene expression occurring after 24 h of infection for genes of profiles 1, 3, and 4 (Fig. 6). The plant is clearly sensing the presence of the nematode within the first 6 h of infection as shown by a rapid increase in gene expression. Rapid stimulation of genes involved in defense is not uncommon in soybean (Droge-Laser et al. 1997; Park et al. 2004b) and these processes can account for as much as 1% of new transcripts within the first 15 min of infection (Durrant et al. 2000). Transcript profiles with similar topology to our profiles 1, 3, and 4 were observed in *Arabidopsis* roots infected with the gall forming nematode *Meloidogyne* spp. (Jammes et al. 2005). However, their time-points only investigated 7, 14, and 21 days post-infection with the decrease in expression observed in profiles (clusters) I, V, VII occurring at 14 days post-infection. However, the difference in plant material (*G. max* vs. *Arabidopsis*), time-points used and nematode type (syncytium forming vs. gall forming) complicate comparing the studies.

We believe that the decrease of genes in profiles 1, 3, and 4 observed at 1 dpi may be the result of the plant sensing and reprogramming itself to somehow cope with the nematode infection as the infection progresses beyond 1 day. Our use of this global analysis of gene expression database during the timecourse of SCN infection allow us to identify genes commonly increased in expression across all time-points, and identify those genes specifically expressed higher at particular stages of infection.

Timecourse microarray analyses identify genes with sustained elevated expression levels

The SCN wounds the root tissue as it migrates to the stele, pierces an endodermal or pericycle cell and creates its feeding site. Further damage occurs later as it expands while feeding. We identified a number of gene transcripts that were elevated at every time-point in our study and that have been reported as associated with the wounding response. Transcripts of genes encoding WRKY6 transcription factor (BM108156), CLB1 (BM108106), Skp1 (BM108118), lipoxygenase (BM108011 and BM108233) and several genes of unknown function were elevated at every time-point in our microarray study. We then confirmed some of the microarray expression data using RT-PCR for WRKY6 transcription factor (BM108156), CLB1 (BM108106), Skp1 (BM108118), TPS (DUP06H06), and EIF4a (BM108249). WRKY genes encode transcription factors that control the plant response to several stresses and are involved in the defense response (Robatzek and Somssich 2001, 2002; Dong et al. 2003). TPS is involved in trehalose synthesis which has been shown to be required at different stages of plant infection by pathogens such as *Magnaporthe grisea* (Foster et al. 2003). CLB1 has some identity with the Ca^{2+}-dependent lipid-binding domains of several proteins (Kiyosue and Ryan 1997). Ca^{2+}-dependent lipid-binding domains have been associated with membrane channeling, signaling, and other cellular processes (Clark and Roux 1995). Our RT-PCR analysis demonstrated CLB1 mRNA accumulation during SCN infection. SKP1 is associated with polyubiquitination, which labels proteins for degradation (Takahashi et al. 2004). In *Lycopersicon esculentum*, SKP1 interacts with the *Fusarium oxysporum* gene FRP1, a gene that is essential for its pathogenicity (Duyvesteijn et al. 2003). EIF4a is the translation factor that interacts with ATP during

protein chain initiation (Seal et al. 1983). Why SCN enhances the accumulation of transcripts of genes involved in protein synthesis is not clear. However, it may be important for SCN pathogenesis or be attributed to the load that SCN imposes on the plant as a sink for amino acids.

Timecourse microarray analyses identify proteins related to defense and stress

Our microarray analyses revealed an increase in the abundance of several transcripts encoding proteins related to defense and stress, including calmodulin (BM108224), phospholipase C (BM108088), metallothionein-like protein (BM108228), chalcone reductase (BM107806) and 4-coumarate CoA ligase (BM107798) throughout most of the time-points studied. Calmodulin participates in signal-transduction mechanisms associated with the defense response. Reymond et al. (2000) noted an elevation of transcripts encoding calmodulin in *Arabidopsis* in response to mechanical wounding and insect feeding. Lee et al. (1995) isolated five isoforms of soybean calmodulin (SCaM1-5) with SCaM-(1–3) protein sequences being almost identical to each other. Heo et al. (1999) demonstrated that specific soybean calmodulin isoforms (SCaM-4 and SCaM-5) are induced upon exposure to fungal elicitors isolated from *Fusarium solani* or *Phytophthora parasitica* var. *nicotianae.* SCaM-4/5 overexpression in tobacco decreased the numbers of lesions caused by *P. parasitica* (Heo et al. 1999). SCaM-4/5 transduces the defense-signaling network into plant resistance through Non-immunity1 (Nim1/Non-expressor of PR genes 1) in transgenic Nim1 mutants of *Arabidopsis* (Park et al. 2004a). Subsequently, Park et al. (2004b) demonstrated binding of a GT-1 like transcription factor on a GT-1 box within the promoter of SCaM-4 during *Pseudomonas syringae* pv *glycinea* attack of soybean W82 suspension culture cells or exposure to salt stress. Our calmodulin isoform (BM108224) that was an incomplete sequence and exhibited an increase in expression on microarrays was identical to SCaM-(1–3) and not the pathogen induced SCaM-4/5. Like calmodulin, phospholipase C activity is dependent upon calcium. Phospholipase C is associated with membranes (Arz and Grambow 1994). Phospholipases are involved in a variety of roles, including the synthesis of antifungal phytooxylipins (Ongena et al. 2004) and jasmonic acid synthesis (Agrawal et al. 2004). Thus, like calmodulin, phospholipase C participates in signal-transduction mechanisms associated with the defense response. Reymond et al. (2000) also noted the elevation in transcripts encoding metallothionein in *Arabidopsis* in response to mechanical wounding and insect feeding. An increase in transcript abundance for metallothionein was also reported by Potenza et al. (2001), when studying the early response of susceptible alfalfa to infection by *Meloidogyne incognita*. Furthermore, they reported increases in transcripts of 4-coumarate:CoA ligase and chalcone synthase, two genes in the phenylpropanoid pathway. At

most time-points we observed elevated transcript levels of chalcone reductase and 4-coumarate CoA ligase of the phenylpropanoid pathway. This supports observations of Reymond et al. (2000) indicating an increase in transcripts encoding phenylalanine ammonia lyase, chalcone synthase, cinnamoyl-CoA reductase, cinnamoyl-CoA reductase, and *O*-methyltransferase 90 min after wounding of *Arabidopsis* rosette leaves with forceps. In a recent review, Gheysen and Fenoll (2002) identified genes encoding chalcone synthase and isoflavone reductase as having increased transcript levels upon the nematode infection, as well as transcripts that encoded lipoxygenase, metallothionein, and WRKY transcription factor, as we noted earlier.

In contrast to the aforementioned genes that are induced at most time-points, some of these defense- and stress-related genes were induced primarily at specific points during infection. At 6 and 12 hpi transcripts that encoded SAM22 (BM107871), Phospholipase D (BM108004 and BM108178) and 12-oxophytodienoate reductase (BM107976) were induced. Phospholipase D was found to be activated upon wounding of castor bean leaves (Ryu and Wang 1996). Phospholipases and 12-oxophytodienoate reductase are members of the octadecanoid pathway that lead to jasmonic acid synthesis.

Timecourse microarray analyses identify elevated levels of genes involved in transcription and translation

The nematode infection and feeding causes numerous changes in the plant root and promotes root metabolism. At 6 and 8 dpi, we identified elevated levels of transcripts encoding a number of genes involved in transcription and translation supporting this view. We observe elevated gene transcripts for ribosomal proteins and initiation factors. These genes include 60S ribosomal protein PO (BM108251), L15 (BM108302), RL15 (BM108302), 40S ribosomal protein (BM108211 and S10 (BM107991), ribosomal protein S20, eukaryotic initiation factors 4A-15 (IEF-4A-a5; BM108249), EIF-3 (CA852991), and numerous others. Furthermore, transcripts of several sugar-related genes were elevated, including those encoding glyceraldehyde 3-phosphate dehydrogenase (GAPDH; BM108242), fructose-bisphosphate aldolase (BM108246), sucrose synthase (BM107809), and sucrose transport protein (BM108083). These may be used for energy metabolism, cell wall rearrangements, and may play many other roles in the plant cell upon SCN infection. Using differential display, Hermsmeier et al. (1998) also identified aldolase transcripts from samples of susceptible soybean root 1 dpi with SCN. GAPDH is induced in potato upon infection with *Phytophthora infestans* and is stimulated by salicylic acid (Laxalt et al. 1996). In peppermint, GAP has been identified as a precursor of isopentenyl diphosphate, used by plants to synthesize isoprenoids, which function in a variety of roles, including communication, defense, hormones, pigments, structural components (Lange et al. 1998).

Timecourse microarray analyses identify elevated levels of unknown genes

Numerous other genes were also induced at some or all time-points, many with no known function. Further characterization of these genes is needed to obtain a better understanding of the susceptibility of Kent towards SCN. However, during SCN infection of soybean roots, transcripts of genes involved in the wound response, signal transduction, transcription, translation, and sugar metabolism are induced.

Identification of elevated levels of genes involved in DNA replication early and later during infection

Another observation made from our experiments was an increase in expression of genes involved in DNA replication. It can be argued that the increases that we observed early and later during infection may be attributed to endoreduplication. Our current understanding is that endoreduplication occurs in syncytia (Gheysen and Fenoll 2002). Experiments aimed at showing cell cycle activity in syncytia have shown increases in *cdc2aAt*, *cdc2bAt*, *CycB1;1*, and *CycA2;1* promoter activity in syncytia (Niebel et al. 1996; de Almeida Engler 1999). However, while their expression may be high, it does not necessarily predict endoreduplication activity. Experiments investigating this demonstrate that a stable association of cyclinB/Cdc2 to DNA replication origins actually prevents endoreduplication in the fission yeast *Schizosaccharomyces pombe* (Wuarin et al. 2002). Cebolla et al. (1999) found that *Medicago* cells exhibiting the highest levels of the mitotic inhibitor ccs52 were differentiating and undergoing endoreduplication. Conversely, antisense suppression of ccs52 decreased the number of endocycles and the volume of the largest cells found in root nodules that typically would undergo endoreduplication. Thus, the complexities involved in DNA replication may warrant a more thorough investigation before it can be stated conclusively that endoreduplication is occurring in syncytia.

Experiments using LCM have isolated syncytia from specific stages of development (Klink et al. 2005). The use of LCM can be used as a means to obtain synchronized populations of syncytia (Klink et al. 2005) and will likely aid in our understanding of the localized events occurring, as syncytia develop into the mature feeding cells of SCN. The use of LCM may also allow us to differentiate localized expression levels occurring within syncytia from expression occurring throughout the root as it perceives and responds to the nematode infection. We will undoubtedly reveal the intricacies that underlie the nematode infection of root tissue as we further explore the use of the technical advancements currently available.

References

Agrawal GK, Tamogami S, Han O, Iwahashi H, Rakwal R (2004) Rice octadecanoid pathway. Biochem Biophys Res Commun 317:1–15

Alkharouf N, Matthews BF (2004) SGMD: the soybean genomics and microarray database. Nucleic Acids Res 32:D398–D400

Alkharouf N, Khan R, Matthews BF (2004) Analysis of expressed sequence tags from roots of resistant soybean infected by the soybean cyst nematode. Genome 47:380–388

Alkharouf N, Jamison C, Matthews BF (2005) Online analytical processing (OLAP): a fast and effective data mining tool for gene expression databases. J Biomed Biotechnol 2:181–188

de Almeida Engler J, De Vleesschauwer V, Burssens S, Celenza JL Jr, Inze D, Van Montagu M, Engler G, Gheysen G (1999) Molecular markers and cell cycle inhibitors show the importance of cell cycle progression in nematode-induced galls and syncytia. Plant Cell 11:793–808

Altschul SF, Madden TL, Schaffer AA, Zhang J, Zhang Z, Miller W, Lipman DJ (1997) Gapped BLAST and PSI-BLAST: a new generation of protein database search programs. Nucleic Acids Res 25:3389–3402

Arz MC, Grambow HJ (1994) Polyphosphoinositide phospholipase C and evidence for inositol-phosphate-hydrolysing activities in the plasma-membrane fraction from light-grown wheat (*Triticum aestivum* L.) leaves. Planta 195:57–62

Bilban M, Buehler LK, Head S, Desoye G, Quaranta V (2002) Normalizing DNA microarray data. Curr Issues Mol Biol 4:57–64

Cebolla A, Vinardell JM, Kiss E, Olah B, Roudier F, Kondorosi A, Kondorosi E (1999) The mitotic inhibitor ccs52 is required for endoreduplication and ploidy-dependent cell enlargement in plants. EMBO J 18:4476–4484

Clark GB, Roux SJ (1995) Annexins of plant cells. Plant Physiol 109:1133–1139

Codd EF, Codd SB, Salley CT (1993) Providing OLAP (on-line analytical processing) to user-analysts: an IT mandate. Technical Report, EF Codd & Associates

Dong J, Chen C, Chen Z (2003) Expression profiles of the *Arabidopsis* WRKY gene superfamily during plant defense response. Plant Mol Biol 51:21–37

Droge-Laser W, Kaiser A, Lindsay WP, Halkier BA, Loake GJ, Doerner P, Dixon RA, Lamb C (1997) Rapid stimulation of a soybean protein-serine kinase that phosphorylates a novel bZIP DNA-binding protein, G/HBF-1, during the induction of early transcription-dependent defenses. EMBO J 16:726–738

Durrant WE, Rowland O, Piedras P, Hammond-Kosack KE, Jones JD (2000) cDNA-AFLP reveals a striking overlap in race-specific resistance and wound response gene expression profiles. Plant Cell 12:963–977

Duyvesteijn RG, van Wijk R, Boer Y, Rep M, Cornelissen BJ, Haring MA (2003) Frp1 is a *Fusarium oxysporum* F-box protein required for pathogenicity on tomato. Mol Microbiol 57:1051–1063

Endo BY (1964) Penetration and development of *Heterodera glycines* in soybean roots and related anatomical changes. Phytopathology 54:79–88

Endo BY (1965) Histological responses of resistant and susceptible soybean varieties, and backcross progeny to entry development of *Heterodera glycines*. Phytopathology 55:375–381

Endo B (1971) Synthesis of nucleic acids at infection sites of soybean roots parasitized by *Heterodera glycines*. Phytopathology 61:395–399

Endo BY (1991) Ultrastructure of initial responses of resistant and susceptible soybean roots to infection by *Heterodera glycines*. Rev Nematol 14:73–94

Foster AJ, Jenkinson JM, Talbot NJ (2003) Trehalose synthesis and metabolism are required at different stages of plant infection by *Magnaporthe grisea*. EMBO J 22:225–235

Gheysen G, Fenoll C (2002) Gene expression in nematode feeding sites. Annu Rev Phytopathol 40:191–219

Grundler FMW, Bockenhoff A (1997) Physiology of nematode feeding and feeding sites. In: Fenoll C, Grundler FMW, Ohl SA (eds) Cellular and molecular aspects of plant–nematode interactions. Kluwer, Dordrecht, pp 107–119

Hermsmeier D, Mazarei M, Baum TJ (1998) Differential display analysis of the early compatible interaction between soybean and the soybean cyst nematode. Mol Plant Microbe Interact 11(12):1258–1263

Heo WD, Lee SH, Kim MC, Kim JC, Chung WS, Chun HJ, Lee KJ, Park CY, Park HC, Choi JY, Cho MJ (1999) Involvement of specific calmodulin isoforms in salicylic acid-independent activation of plant disease resistance responses. Proc Natl Acad Sci USA 96:766–771

Hegde P, Qi R, Abernathy K, Gay C, Dharap S, Gaspard R, Hughes JE, Snesrud E, Lee N, Quackenbush J (2000) A concise guide to cDNA microarray analysis. Biotechniques 29:548–556

Jammes F, Lecomte P, de Almeida-Engler J, Bitton F, Martin-Magniette ML, Renou JP, Abad P, Favery B (2005) Genome-wide expression profiling of the host response to root-knot nematode infection in *Arabidopsis*. Plant J 44:447–458

Jung C, Wyss U (1999) New approaches to control plant parasitic nematodes. Appl Microbiol Biotechnol 51:439–446

Kawasaki S, Borchert C, Deyholos M, Wang H, Brazille S, Kawai K, Galbraith D, Bohnert HJ (2001) Gene expression profiles during the initial phase of salt stress in rice. Plant Cell 13:889–905

Khan R, Alkharouf N, Beard HS, MacDonald M, Chouikha I, Meyer S, Grefenstette J, Knap H, Matthews BF (2004) Resistance mechanisms in soybean: gene expression profile at an early stage of soybean cyst nematode invasion. J Nematol 36:241–248

Kiegle E, Moore CA, Haseloff J, Tester MA, Knight MR (2000) Cell-type-specific calcium responses to drought, salt and cold in the *Arabidopsis* root. Plant J 23:267–278

Kiyosue T, Ryan CA (1997) A novel gene of tomato preferentially expressed in fruit encodes a protein with a Ca^{2+}-dependent lipid-binding domain. Plant Mol Biol 35:969–972

Klink VP, MacDonald M, Alkharouf N, Matthews BF (2005) Laser capture microdissection (LCM) and expression analyses of *Glycine max* (soybean) syncytium containing root regions formed by the plant pathogen *Heterodera glycines* (soybean cyst nematode). Plant Mol Biol 59:969–983

Lange BM, Wildung MR, McCaskill D, Croteau R (1998) A family of transketolases that directs isoprenoid biosynthesis via a mevalonate-independent pathway. Proc Natl Acad Sci USA 95:2100–2104

Laxalt AM, Cassia RO, Sanllorenti PM, Madrid EA, Andreu AB, Daleo GR, Conde RD, Lamattina L (1996) Accumulation of cytosolic glyceraldehydes-3-phosphate dehydrogenase RNA under biological stress conditions and elicitor treatments in potato. Plant Mol Biol 30:961–972

Lee SH, Kim JC, Lee MS, Heo WD, Seo HY, Yoon HW, Hong JC, Lee SY, Bahk JD, Hwang I, Cho MJ (1995) Identification of a novel divergent calmodulin isoform from soybean which has differential ability to activate calmodulin-dependent enzymes. J Biol Chem 270:21806–21812

Mahalingam R, Wang G, Knap HT (1999) Polygalacturonase and polygalacturonase inhibitor protein: gene isolation and transcription in *Glycine max–Heterodera glycines* interactions. Mol Plant Microbe Interact. 12:490–498

Mujer CV, Andrews DL, Manhart JR, Pierce SK, Rumpho ME (1996) Chloroplast genes are expressed during intracellular symbiotic association of *Vaucheria litorea* plastids with the sea slug *Elysia chlorotica*. Proc Natl Acad Sci USA 93:12333–12338

Niebel A, Heungens K, Barthels N, Inze C, Van Montagu M, Gheysen G (1995) Characterization of a pathogen-induced potato catalase and its systemic expression upon nematode and bacterial infection. Mol Plant Microbe Interact 8:371–378

Niebel A, de Almeida Engler J, Hemerly A, Ferreira P, Inze D, Van Montagu M, Gheysen G (1996) Induction of cdc2a and cyc1At expression in *Arabidopsis thaliana* during early phases of nematode-induced feeding cell formation. Plant J 10:1037–1043

Ongena M, Duby F, Rossignol F, Fauconnier ML, Dommes J, Thonart P (2004) Stimulation of the lipoxygenase pathway is associated with systemic resistance induced in bean by a non-pathogenic Pseudomonas strain. Mole Plant Path Interact 17:1009–1018

Oztur ZN, Talame V, Deyholos M, Michalowski CB, Gozukirmizi DW, Tuberosa R, Bohnert HJ (2002) Monitoring large-scale changes in transcript abundance in drought- and salt-stressed barley. Plant Mol Biol 48:551–573

Park CY, Heo WD, Yoo JH, Lee JH, Kim MC, Chun HJ, Moon BC, Kim IH, Park HC, Choi MS, Ok HM, Cheong MS, Lee SM, Kim HS, Lee KH, Lim CO, Chung WS, Cho MJ (2004a) Pathogenesis-related gene expression by specific calmodulin isoforms is dependent on NIM1, a key regulator of systemic acquired resistance. Mol Cells 18:207–213

Park HC, Kim ML, Kang YH, Jeon JM, Yoo JH, Kim MC, Park CY, Jeong JC, Moon BC, Lee JH, Yoon HW, Lee SH, Chung WS, Lim CO, Lee SY, Hong JC, Cho MJ (2004b) Pathogen- and NaCl-induced expression of the SCaM-4 promoter is mediated in part by a GT-1 box that interacts with a GT-1-like transcription factor. Plant Physiol 135:2150–2161

Potenza C, Thomas SH, Sengupta-Gopalan C (2001) Genes induced during early response to *Meloidogyne incognita* in roots of resistant and susceptible alfalfa cultivars. Plant Sci 161:289–299

Puthoff DP, Nettleton D, Rodermel SR, Baum TJ (2003) *Arabidopsis* gene expression changes during cyst nematode parasitism revealed by statistical analyses of microarray expression profiles. Plant J 33:911–921

Reymond P, Weber H, Damond M, Farmer EE (2000) Differential gene expression in response to mechanical wounding and insect feeding in *Arabidopsis*. Plant Cell 12:707–719

Robatzek S, Somssich IE (2001) A new member of the *Arabidposis* WRKY transcription factor family, *At*WRKY6 is associated with both senescence- and defence-related processes. Plant J 28:123–133

Robatzek S, Somssich IE (2002) Targets of *At*WRKY6 regulation during plant senescence and pathogen defense. Genes Dev 16:1139–1149

Ryu SB, Wang X (1996) Activation of phospholipase D and the possible mechanism of activation in wound-induced lipid hydrolysis in castor bean leaves. Biochim Biophys Acta 1303:243–250

Seal SN, Schmidt A, Marcus A (1983) Eukaryotic initiation factor 4A is the component that interacts with ATP in protein chain initiation. Proc Natl Acad Sci USA 80:6562–6565

Schaffer R, Landgraf J, Acerbi M, Simon V, Larson M, Wisman E (2001) Microarray analysis of diurnal and circadian-regulated genes in *Arabidopsis*. Plant Cell 13:113–123

Schenk PM, Kazan K, Wilson I, Anderson JP, Richmond T, Somerville SC, Manners JM (2000) Coordinate plant defense responses in *Arabidopsis* revealed by microarray analysis. Proc Natl Acad Sci USA 97(21):11655–11660

Seki M, Narusaka M, Abe H, Kasuga M, Yamaguchi-Shinozaki K, Carcini P, Hayashizaki Y, Shinozaki K (2001) Monitoring the expression pattern of 1300 *Arabidopsis* genes under drought and cold stresses using a full-length cDNA microarray. Plant Cell 13:61–72

Takahashi N, Kuroda H, Kuromori T, Hirayama T, Seki M, Shinozaki K, Shimada H, Matsui M (2004) Expression and interaction analysis of *Arabidopsis Skp1*-related genes. Plant Cell Physiol 45:83–91

The Gene Ontology Consortium (2004) The Gene Ontology (GO) database and informatics resource. Nucleic Acids Res 32:D258–D261

Tomkins JP, Mahalingam R, Smith H, Goicoechea JL, Knap HT, Wing RA (1999) A bacterial artificial chromosome library for soybean PI 437654 and identification of clones associated with cyst nematode resistance. Plant Mol Biol 41:25–32

Tusher V, Tibshirani R, Chu C (2001) Significance analysis of micro-arrays applied to ionizing radiation response. Proc Natl Acad Sci USA 98:5116–5121

Vaghchhipawala Z, Bassuner R, Clayton K, Lewers K, Shoemaker R, Mackenzie S (2001) Modulations in gene expression and mapping of genes associated with cyst nematode infection of soybean. Mol Plant Microbe Interact 14:42–54

Vaghchhipawala ZE, Schlueter JA, Shoemaker RC, Mackenzie SA (2004) Soybean FGAM synthase promoters direct ectopic nematode feeding site activity. Genome 47:404–413

Van der Eycken W, de Almeida Engler J, Inze D, Montagu M, Gheysen G (1996) A molecular study of root-knot nematode-induced feeding sites. Plant J 9:45–54

Vodkin LO, Khanna A, Shealy R, Clough SJ, Gonzalez DO, Philip R, Zabala G, Thibaud-Nissen F, Sidarous M, Stromvik MV, Shoop E, Schmidt C, Retzel E, Erpelding J, Shoemaker RC, Rodriguez-Huete AM, Polacco JC, Coryell V, Keim P, Gong G, Liu L, Pardinas J, Schweitzer P (2004) Microarrays for global expression constructed with a low redundancy set of 27,500 sequenced cDNAs representing an array of developmental stages and physiological conditions of the soybean plant. BMC Genomics 5:73–91

Wuarin J, Buck V, Nurse P, Millar JB (2002) Stable association of mitotic cyclin B/Cdc2 to replication origins prevents endoreduplication. Cell 111:419–431

Wrather JA, Stienstra WC, Koenning SR (2001) Soybean disease loss estimates for the United States from 1996 to 1998. Can J Plant Pathol 23:122–131

Yang YH, Dudoit S, Luu P, Lin DM, Peng V, Ngai J, Speed TP (2002) Normalization of cDNA microarray data: a robust composite method addressing single and multiple slide systematic variation. Nucleic Acid Res 30(4):e15